

***Pseudomonas aeruginosa* Theft Biofilm Require Host Lipids of Cutaneous Wound**

Mithun Sinha, PhD^{1,*,#}, Nandini Ghosh, PhD^{1,*}, Dayanjan S Wijesinghe, PhD², Shomita S. Mathew-Steiner, PhD¹, Amitava Das, PhD¹, Kanhaiya Singh, PhD¹, Mohamed El Masry, MD PhD^{1,3}, Savita Khanna, PhD¹, Hiroyuki Inoue⁴, Katsuhisa Yamazaki, PhD⁴, Manabu Kawada, PhD⁴, Gayle M Gordillo, MD¹, Sashwati Roy, PhD¹, Chandan K Sen, PhD^{1,#}

¹Indiana Center for Regenerative Medicine and Engineering, Department of Surgery, IU Health Comprehensive Wound Center, Indiana University School of Medicine, Indianapolis, Indiana, USA

²Department of Pharmacotherapy and Outcomes Science, School of Pharmacy, Virginia Commonwealth University, Richmond, Virginia, USA

³Department of Plastic and Reconstructive Surgery, Zagazig University, Egypt

⁴Institute of Microbial Chemistry, Microbial Chemistry Research Foundation, Tokyo, Japan

*These authors contributed equally.

† Corresponding Authors: Chandan K. Sen, PhD; cksen@iu.edu

Mithun Sinha, PhD; mitsinha@iu.edu

Address: 975 W Walnut St, Medical Research Library Building,
Indiana University School of Medicine, Indianapolis, IN 46202.
Tel. 317 278 2636; Fax. 317 278 2708

Short Title: Theft biofilm in skin wound

This is an open-access article distributed under the terms of the Creative Commons Attribution-Non Commercial-No Derivatives License 4.0 (CCBY-NC-ND), where it is permissible to download and share the work provided it is properly cited. The work cannot be changed in any way or used commercially without permission from the journal.

MINI ABSTRACT

In cutaneous wounds, *Pseudomonas aeruginosa* forms pathogenic theft biofilm. Sinha *et al* demonstrate that such biofilm severity relies on the theft of host lipids causing potent induction of bacterial ceramidase. Skin lipid homeostasis is disrupted such that the site of wound repair is deficient in barrier function exacerbating host pathology.

ABSTRACT

Objective: This work addressing complexities in wound infection, seeks to test the reliance of bacterial pathogen *Pseudomonas aeruginosa* (PA) on host skin lipids to form biofilm with pathological consequences.

Background: PA biofilm causes wound chronicity. Both CDC as well as NIH recognizes biofilm infection as a threat leading to wound chronicity. Chronic wounds on lower extremities often lead to surgical limb amputation.

Methods: An established pre-clinical porcine chronic wound biofilm model, infected with PA or *Pseudomonas aeruginosa* ceramidase mutant (PA Δ Cer) was used.

Results: We observed that bacteria drew resource from host lipids to induce PA ceramidase expression by three orders of magnitude. PA utilized product of host ceramide catabolism to augment transcription of PA ceramidase. Biofilm formation was more robust in PA compared to PA Δ Cer. Downstream products of such metabolism such as sphingosine and sphingosine-1-phosphate were both directly implicated in the induction of ceramidase and inhibition of PPAR δ , respectively. PA biofilm, in a ceramidastin-sensitive manner, also silenced PPAR δ *via* induction of miR-106b. Low PPAR δ limited ABCA12 expression resulting in disruption of skin lipid homeostasis. Barrier function of the wound-site was thus compromised.

Conclusion: This work demonstrate that microbial pathogens must co-opt host skin lipids to unleash biofilm pathogenicity. Anti-biofilm strategies must not necessarily always target the microbe and targeting host lipids at risk of infection could be productive. This work may be viewed as a first step, laying fundamental mechanistic groundwork, towards a paradigm change in biofilm management.

INTRODUCTION

Bacterial biofilms complicate wound healing¹⁻³. The Center for Disease Control estimates that 65% of all human infections are caused by bacteria with biofilm phenotype and the National Institutes of Health estimates that this number is closer to 80%⁴. Majority of chronic wounds are known to be infected by *Pseudomonas aeruginosa* (PA). Importantly, of all bacterial biofilm aggregates, those of PA are the largest⁵. PA infection is known to cause wound chronicity⁶. PA is equipped with repertoire of virulence determinants and a complex regulatory network of intracellular and intercellular signals⁷ that allow the bacteria to adapt, thrive and escape host defense⁸. They can live as free-living planktonic cells or as members of a biofilm community and have the exceptional ability to translate microbial signals and environmental cues into niche-specific processes⁹.

In the setting of host-microbe interaction, mechanistic underpinnings of biofilm infection are contextual and depend on the host tissue microenvironment. In this work, microbial biofilm involving larceny of host factors towards bolstering of underlying formative mechanisms, and worsening of host pathogenicity, is viewed as theft biofilm. Local tissue biochemistry as well as immune defense responses both influence such mechanisms¹⁰. Thus, translationally relevant understanding of wound biofilm infection may only be acquired from immune-competent preclinical models especially when delineation of time-dependent cascade of events is of interest¹⁻³. Such approach enables the investigation of bacteria of clinical interest, such as PA AN17 strain¹¹. Bacteria produce lipases which hydrolyze host esters of glycerol with fatty acids. In a skin wound microenvironment this is of outstanding significance. Epidermal lipids are a mixture of ceramides, free fatty acids and cholesterol. Ceramides are a major lipid constituent, accounting for 40% - 50% of the cutaneous lipids by weight¹². Exogenous fatty acids are known to contribute to PA pathogenicity by altering bacterial membrane phospholipid structure, membrane permeability, virulence phenotypes and consequent stress responses that augment survival and persistence of these bacteria¹³. In this study, we sought to investigate the interaction between host skin lipids and bacterial factors capable of metabolizing them with the overall goal to understand how such interaction may determine biofilm formation. Findings of this work lend credence to a “theft biofilm” paradigm wherein massive induction of PA ceramidase by host skin lipids establish a loop whereby host factors are “stolen” to induce bacterial ceramidase transcription towards impaired functional wound closure.

METHODS

Detailed methodology in Supplementary Information, <http://links.lww.com/SLA/D496> (Supp inf)

Animals. All animal (pig) experiments were approved by the Indiana University School of Medicine Institutional Animal Care and Use Committee (SoM-IACUC) and Ohio State University Institutional Laboratory Animal Care and Use Committee (ILACUC) under protocols 18048 and 2008A0012 respectively.

Bacterial strains. *Pseudomonas aeruginosa* wild type strain (PA_{wt}), *Pseudomonas aeruginosa* ceramidase mutant (PA_{Δcer}) were grown on Luria Agar (LA) plates or Luria broth with low sodium chloride (LBNS) at 37°C^{1,2}.

Porcine Full Thickness Burn and Biofilm Wound Model. Domestic Yorkshire female pigs were wounded and infected to establish chronic wound biofilm model as described previously^{1-3,14}. Eight full thickness burn wounds were made and infected with culture comprising of PA_{wt}, or PA_{Δcer} strains (CFU10⁵/ml) with *Acinetobacter baumannii* (AB) (CFU10⁶/ml) in both groups or allowed to be colonized by skin microflora and referred as spontaneously infected (SI)². Wounds were followed up to 56 days post infection. Details in *Supp inf*.

Scanning Electron Microscope Imaging. Sample processing and imaging was performed as described previously¹. Details in *Supp inf*.

Trans-epidermal Water Loss (TEWL) measurement. DermaLab Combo™ (cyberDERM inc., Broomall, PA) was used to measure the trans-epidermal water loss from the wounds². TEWL was measured in g (m²)⁻¹ h⁻¹.

Bacterial Ceramidase activity. *Pseudomonas* ceramidase activity assay was adapted from Ohnishi *et al*¹⁵. Details in *Supp inf*.

Lipidomic analyses using LC ESI-MS/MS. Targeted and untargeted analysis of the sphingolipidome was undertaken as previously described^{16,17,18}. Details in *Supp inf*.

Lipidomic analysis of Sphingosine-1-Phosphate (S-1-P). Porcine wound edge tissue pulverized samples were spiked with 20μl of ceramide/sphingolipid mixture I (Avanti) with 0.5 nmol of d17:1-P. The lipids were extracted using a modified Bligh and Dyer method¹⁷. Quantitation was based on Multiple Reaction Monitoring (MRM). Details in *Supp inf*.

In vitro Pseudomonas biofilm model. *In vitro* biofilm culture on polycarbonate membrane was adapted from Zhao *et al.*, 2010¹⁹. *In vitro* biofilm was grown on a polycarbonate membrane (PCM) by inoculating PA_{wt}, or PA_{Δcer} bacteria cells (CFU10⁵/ml) with or without porcine skin lipids for 24h. Details in *Supp inf*.

Immunohistochemistry. Immunohistochemical staining of the frozen sections and immunocytochemistry were performed using standard procedures² Antibodies listed in **Table S3**, <http://links.lww.com/SLA/D496>.

Nile Red Staining. The OCT embedded wound tissue sections were stained with Nile red as described previously²⁰. Details in *Supp inf*.

Wheat-germ agglutinin staining. The PCM disc with *in-vitro* bacteria biofilm were WGA - Alexa Fluor™ 488 Conjugate as described previously²¹. Details in *Supp inf*.

Western Blot analyses. Western blot was performed using antibodies against anti-PPARδ and anti-CerS3. β-actin was used as housekeeping. Antibodies listed in **Table S3**, <http://links.lww.com/SLA/D496>.

PPARδ trans-activity assay. Human keratinocytes cells were treated with 5μmol of long chain ceramides, C18:0 and C 24:0 (Avanti) and collected 48 h post treatment. Nuclear protein was extracted using Nuclear Extraction Kit (RayBiotech) and PPARδ trans-activity was measured using PPAR delta Transcription Factor Assay Kit (abcam) as per manufacturer's instructions. Details in *Supp inf*.

DNMT3B activity assay. Human keratinocytes cells were treated with 5 μ mol S-1-P (Avanti) for 48h. Cells were collected and DNMT3B activity was measured using EpiQuik DNMT3B Activity/Inhibitor Screening Assay Core Kit (Epigentek) according to manufacturer's instructions and using recombinant DNMT3B protein, (Active motif) as a positive control. Details in *Supp inf*.

PPAR δ promoter assay. PPAR δ promoter assay was done as follows. mNP-Luc (PPARdelta promoter) (Addgene) reporter construct was used. Human keratinocytes cells were co-transfected with the PPAR δ promoter reporter construct and 5 μ mol of C:18 and C:24. Luciferase assay and normalization was performed using the dual-luciferase reporter assay system (Promega). Data are presented as the ratio of firefly: renilla².

miR-Target 3'-UTR reporter assay. Human keratinocytes were transfected with miRIDIAN mimic-miR-106b followed by transfection with miR target PPAR δ -3'-UTR plasmid (NM_006238) or CerS3-3'-UTR plasmid (NM_178842). Luciferase assay and quantification done as mentioned above. Details in *Supp inf*.

miRNA delivery. Transfection of human keratinocytes cells was performed as described². Details in *Supp inf*.

Bisulfite Conversion of DNA sequencing of PPAR δ Promoter. Bisulfite conversion of DNA and sequencing of S-1-P transfected human keratinocytes was performed as described previously²². Primers for sequencing PPAR δ promoter region listed in **Table S2**, <http://links.lww.com/SLA/D496>. Details in *Supp inf*.

Quantification and statistical analysis

The data analysis was performed using student's t-test (two-tailed) presented as mean \pm SEM. Mean, SEM and student *t*-test analyses was done using in-built function in Microsoft Excel 2010. Comparisons among multiple groups were tested using ANOVA in-built function in GraphPad Prism 9.1.2. $p < 0.05$ was considered statistically significant.

RESULTS

Wound Biofilm Infection Depletes Host Skin Ceramides

In an established pre-clinical porcine chronic wound biofilm model² (**Fig. 1A**, **Table S1**, <http://links.lww.com/SLA/D496>), the expression of PA ceramidase was induced by three orders of magnitude on day 7 following infection with PA_{wt} (**Fig. 1B**). Control wounds were not subjected to induced infection and were allowed to be colonized by natural skin microflora. These wounds are referred to as spontaneously infected (SI)². Bacterial ceramidase is known to cause breakdown of host ceramides¹⁵. To determine the significance of PA ceramidase a ceramidase deficient PA Δ Cer was studied. The loss of ceramidase (*bcdase*) gene in the mutant bacterial strain was validated using qRT PCR (**Fig. S1A**, <http://links.lww.com/SLA/D496>). Loss of ceramidase activity was evident in PA Δ Cer as measured by thin layer chromatography (TLC) using a fluorescent ceramide analog (**Fig. 1C**). PA and AB infection was confirmed by CFU assay on *Pseudomonas aeruginosa* selection agar and *Acinetobacter* selection agar (**Figs. S1B**, <http://links.lww.com/SLA/D496>, **S2**, <http://links.lww.com/SLA/D496>).

To identify bacterial species and their abundance, a 16S rRNA (variable region) next generation sequencing (NGS) was performed. PA infection was further confirmed on the basis of NGS sequencing (**Fig. S1C**, <http://links.lww.com/SLA/D496>). Though the initial infection was polymicrobial (PA+AB), over time PA prevailed as dominant biofilm species (**Figs. S1C**, <http://links.lww.com/SLA/D496>, **S2E-F**, <http://links.lww.com/SLA/D496>) as determined by NGS and CFU assays (**Figs. S1C**, <http://links.lww.com/SLA/D496>, **S2**, <http://links.lww.com/SLA/D496>). To test whether the reported effects are causatively linked to AB infection, group of pigs that was infected with PA_{wt} alone, and another group was infected with AB alone. Ceramide abundance was measured in the wound tissue d56 post-infection. Ceramide depletion was limited to wounds infected with PA and was not evident in response to AB infection (**Fig. S3A-B**, <http://links.lww.com/SLA/D496>). These data are consistent with our published IHC/MALDI-TOF studies characterizing pig wound infection^{1,3}. The formation of bacterial biofilm aggregates was validated using scanning electron microscopy (SEM) and staining with PA biofilm matrix component Pel-specific *Wisteria floribunda* lectin (WFL) staining²³ (**Fig. S1D**, <http://links.lww.com/SLA/D496>, **S1E-F**, <http://links.lww.com/SLA/D496>).

Biofilm-dependent loss of skin ceramide was evident in PA_{wt}, but not in PA_{ΔCer} (**Fig. 1D-E**). *In vitro* studies identified that exposure to host skin lipids potently induced *bcdase* in PA_{wt}; such induction was attenuated in PA_{wt} exposed to depleted skin lipids (**Fig. S1G**, <http://links.lww.com/SLA/D496>). Inducible *bcdase* was associated with the induction of the *Pseudomonas* SphR gene (**Fig. S1H-I**, <http://links.lww.com/SLA/D496>). SphR is known to function as the transcriptional activator of *bcdase*²⁴.

Biofilm-dependent loss of skin ceramides was characterized employing a lipidomics approach. Nineteen long-chain cutaneous ceramides were observed to be depleted in response to biofilm infection by PA_{wt}, but not PA_{ΔCer} (**Fig. 1F, S4A-S**, <http://links.lww.com/SLA/D496>). Principal component analyses (PCA) revealed that the abundance of cutaneous ceramides in response to PA_{wt} was statistically distinct from the cluster of cutaneous ceramide levels in response to PA_{ΔCer} and sham exposure (**Fig. 1G**). Mechanistic studies addressing the loss of keratinocyte ceramide following PA_{wt} biofilm infection were conducted *in vitro* (**Fig. S4T**, <http://links.lww.com/SLA/D496>). Ceramidastin, an inhibitor of PA ceramidase²⁵, rescued keratinocyte ceramide against loss caused by PA_{wt} biofilm infection (**Fig. S4U**, <http://links.lww.com/SLA/D496>). Consistent data on rescue of ceramides by ceramidastin was observed in *ex vivo* studies on extracted skin lipids treated with biofilm-conditioned media (**Fig. S5A-L**, <http://links.lww.com/SLA/D496>).

Wounds in all three groups of infection (SI, PA_{wt} and PA_{ΔCer}) were studied over a period of 56 days. During this period, all of these wounds were completely closed as evident by wound planimetry (**Fig. S5M**, <http://links.lww.com/SLA/D496>) as well as histology (**Fig. 1H, S3C**, <http://links.lww.com/SLA/D496>). In such experimental setting, we sought to determine the functional significance of biofilm-dependent depletion of skin ceramides. Skin barrier integrity was studied by measuring trans-epidermal water loss (TEWL). Under conditions of PA_{wt} biofilm infection, depletion of skin ceramides was associated with elevated TEWL (**Fig. 1I**). Such impairment in skin barrier function was not observed in response to PA_{ΔCer} (**Fig. 1I**).

These findings establish a causal relationship between induction of *bcdase* and inability of the repaired skin to restore barrier integrity.

Skin lipids augment biofilm via bcdase

Study of skin tissue extract, native or lipid-depleted (**Fig. S6A-B**, <http://links.lww.com/SLA/D496>), demonstrated clear role of lipids in augmenting biofilm formation. To test the significance of breakdown of skin ceramides on biofilm formation, extracted lipids were added to bacteria that were sufficient or deficient in *bcdase*. Addition of skin lipid extract markedly enhanced biofilm formation in PA_{wt} as measured by SEM and EPS staining (**Fig. 2A-C**). Such augmentation was blunted in PA_{ΔCer} (**Fig. 2D-E**). This pointed towards a likely role of skin ceramide degradation products in biofilm formation (**Figs. 2F, S6C-G**, <http://links.lww.com/SLA/D496>). During biofilm formation, bacteria use quorum sensing (QS) to coordinate behaviors such as antibiotic resistance²⁶. In PA, QS is driven by a series of small molecule receptors, including the master QS systems *mvfR* which is also known as *pqsR* and *rhlR*²⁷. In line with structural observations on biofilm aggregates, the expression of *pqsR*, and *rhlR*, was markedly high in PA_{wt} biofilm treated with host lipids as compared to PA_{ΔCer} under the same treatment conditions (**Fig. 2G, H**). An increased growth of PA_{ΔCer} was observed (**Fig. S6H**, <http://links.lww.com/SLA/D496>). This is in consistent with the in vivo observation where PA_{ΔCer} exhibited faster growth. Though, PA_{wt} was a comparative slow grower in presence of host, it exhibited increased biofilm formation as documented through blue phenazine (pyocyanin) formation, WGA staining and crystal violet staining (**Fig. 2B, S6I**, <http://links.lww.com/SLA/D496>) and increased expression of *pqsR* gene (**Fig. 2H**). *PqsR/mvfR* is known to be required for pyocyanin formation²⁸. Pyocyanin contributes to biofilm formation by facilitating extracellular DNA binding to PA²⁹. These data thus demonstrated that the microbial pathogens are not capable of mounting the complex threat in isolation and that they must co-opt host skin lipids to generate complex biofilms.

Wound biofilm downregulates host skin CerS3 and depletes dihydroceramide

Skin ceramide homeostasis relies on a CerS3-dependent biosynthetic pathway that produces long-chain ceramides³⁰ (**Fig. 3A**). Wound biofilm infection compromised ceramide biosynthesis by downregulating CerS3 expression in the PA_{wt} infected wounds, but not in PA_{ΔCer} (**Fig. 3B, S7A**, <http://links.lww.com/SLA/D496>). Blunted cutaneous CerS3 expression was associated with depletion of long-chain dihydroceramide levels in the porcine skin tissue exposed to PA_{wt} infection (**Fig. 3C**). To determine the presence of PA biofilm, cyclic di-GMP was used as a surrogate marker in the wound fluids from chronic wound patients. Consistent with our findings from pre-clinical porcine studies, the investigation of wound fluid from chronic wound patients revealed tight correlation between lowering of long-chain dihydroceramide levels with elevated levels of a PA biofilm marker cyclic di-GMP (**Fig. 3D-F, S7B-H**, <http://links.lww.com/SLA/D496>). Thus, PA biofilms, as marked by diGMP, was associated with lower levels of dihydroceramide.

Our previous work identified miR-106b as biofilm-inducible in wound-edge skin tissue with a pathogenic role². In this work, miR-106b was induced in response to biofilm infection caused by PA_{wt}, but not by PA_{ΔCer} (**Fig. 3G-H**). CerS3 is subject to post-transcriptional gene silencing by miRNA. RNAHybrid™ analyses revealed that the 3'-UTR of CerS3 is likely to be targeted

by miR-106b (**Fig. 3I-J**). Biological validation of such prediction was conducted in human keratinocytes. Delivery of miR-106b mimic significantly lowered CerS3 3'-UTR reporter activity (**Fig. 3K, S7I**, <http://links.lww.com/SLA/D496>). Consistent with this finding, miR-106b mimic decreased CerS3 protein expression (**Fig. 3L**).

Arrest of PPAR δ activity following biofilm-dependent ceramide depletion

In the peroxisome proliferator-activated receptor (PPAR) family of transcription factors, PPAR δ specifically is ceramide-sensitive³¹. In biofilm-affected ceramide-depleted tissue, PPAR δ expression was downregulated. Such effect was not observed under conditions of PA Δ Cer infection pointing towards a causative role of skin ceramide depletion (**Fig. 4A-D**). To address the underlying mechanisms, studies on human keratinocyte biofilm infection were conducted. Consistent with findings from porcine studies, biofilm infection blunted PPAR δ expression (**Fig. 4E**). Such effect was rescued in the presence of the PA ceramidase inhibitor, ceramidastin (**Fig. 4F**). Skin ceramides are primarily long-chain (\geq C18). Thus, C18 and C24 ceramides were tested for their ability to regulate PPAR δ function. In human keratinocytes, these long-chain ceramides induced PPAR δ transactivation (**Fig. 4G-H**) as well as transcription (**Fig. 4I, S8A**, <http://links.lww.com/SLA/D496>). PPAR δ agonist GW501516 increased expression of CerS3 (**Fig. S8B**, <http://links.lww.com/SLA/D496>) whereas its antagonist GSK0660 blunted the expression of CerS3 (**Fig. S8C**, <http://links.lww.com/SLA/D496>) in keratinocytes. These findings constitute evidence demonstrating direct regulation of PPAR δ by ceramides in keratinocytes.

Spingosine-1-phosphate methylates PPAR δ promoter

Cutaneous ceramide is degraded to sphingosine by bacterial ceramidase¹⁵. Sphingosine is phosphorylated to sphingosine-1 phosphate (S-1-P) which is a bioactive lipid and can epigenetically downregulate gene regulation³². Thus, a plausible role of S-1-P in regulating PPAR δ in our experimental systems was tested. In the porcine pre-clinical model of wound biofilm infection elevated levels of S-1-P was detected following PA_{wt}, but not PA Δ Cer, infection (**Fig. 4J**). This finding indicated that the detected S-1-P was a breakdown product of skin ceramide acted upon by *bedase*. Under standard culture conditions when human keratinocytes were treated with the bioactive sphingolipid S-1-P, gene expression of PPAR δ was blunted (**Fig. 4K**). To determine whether such downregulation of PPAR δ was epigenetically regulated, CpG methylation of the PPAR δ promoter was studied. S-1-P caused promoter methylation (**Fig. 4L**). Such increased PPAR δ promoter methylation was associated with augmented catalytic activity of DNA methyl transferase 3B (DNMT3B; **Fig. 4M**). A survey of the effects S-1-P on epigenetic regulators unveiled broader effects on gene expression favoring DNA methylation and histone deacetylation (**Fig. S8D-N**, <http://links.lww.com/SLA/D496>). Induction of miR-106b by S-1-P constitutes an additional epigenetic mechanism by which S-1-P may attenuate PPAR δ (**Fig. S8O**, <http://links.lww.com/SLA/D496>).

PPAR δ is a novel target of biofilm induced miR-106b

The search for PPAR δ targeting miRs, that were also biofilm-inducible, led to the identification of miR-106b as a candidate (**Fig. 5A**). Delivery of miR-106b mimic compromised PPAR δ

levels both at mRNA (**Fig. 5B**) and protein levels (**Fig. 5C**). PPAR δ was further validated as a target for miR-106b by 3'UTR luciferase reporter assay (**Fig. 5D**). Systematic studies thus established PPAR δ as a target of biofilm inducible miR-106b in keratinocytes.

Epidermal lipid transporter ABCA12 is compromised following wound biofilm infection

Skin ceramides are responsible for an estimated 50% of all cutaneous lipids³³. Other skin lipids play a significant role in enabling skin barrier function³⁴. These two are known to interactively maintain skin health³⁵. ABCA12, the transcription of which is PPAR δ -dependent (**Fig. S9A-B**, <http://links.lww.com/SLA/D496>), is an epidermal keratinocyte lipid transporter³⁶. Wound-site ABCA12 expression was attenuated in response to biofilm infection by PA_{wt}, but not SI or PA Δ Cer (**Fig. 6A-D, S9C**, <http://links.lww.com/SLA/D496>). Such downregulation of ABCA12 was associated with overt changes in skin lipid distribution. At the wound-site epidermis, levels of polar and neutral lipids were sharply lower in response to biofilm infection by PA_{wt}, but not by SI or PA Δ Cer (**Fig. 6E**). Mechanistic follow up studies on human keratinocytes revealed that loss of ABCA12 in response to biofilm infection by PA_{wt} was prevented by ceramidastin demonstrating that the loss was caused by a breakdown product of keratinocyte ceramide acted upon by *bcdase* (**Fig. 6F**). Such finding was consistent with the prevention of loss of ABCA12 in response to infection by PA Δ Cer (**Fig. 6B-C**). **Fig. 7** presents a summary of mechanisms gleaned based on this work.

DISCUSSION

Armed with a wide range of lipid metabolizing inducible enzymes, PA is known to exploit host lipids to facilitate host cell binding and to evade host immune defenses³⁷. In macrophages of the innate immune defense system, PA bolsters acid sphingomyelinase activity causing release of host lipid ceramides producing sphingolipid-rich rafts which helps internalization of PA³⁸. In the lungs, PA lipoxygenase (pLoxA) oxidize host arachidonic acid – phosphatidylethanolamine to cause bronchial epithelial ferroptosis and establish airway biofilm³⁹. The notion that host lipids may be pre-emptively primed to compromise the ability of pathogenic microbes to co-opt them emerges as result. Induction of bacterial ceramidases by three orders of magnitude in PA biofilm-infected wound tissue, as reported in this work, called for a systematic investigation testing its significance in the healing response in biofilm affected wounds.

The Wound Healing Society recommends the study of porcine model as the most relevant preclinical model of skin wound healing⁴⁰. The current work is based on the study of an established model of chronic wound biofilm infection in immune-competent pigs *in vivo*^{1,2}. The approach results in the establishment of an induced polymicrobial wound biofilm comprising of *Pseudomonas aeruginosa* (PA) and *Acinetobacter baumannii*. Non-infected skin wounds colonized by normal skin flora of the porcine served as baseline control and were referred to as spontaneous infection (SI). Prior publications using this model revealed that PA establishes itself as the dominant strain as the wound becomes chronic¹⁻³.

Skin serves the primary function of affording barrier defense. Loss of skin barrier increases vulnerability to infection and allergens⁴¹. Compromised skin barrier function is also associated with atopic dermatitis, psoriasis, contact dermatitis, and some specific genetic disorders⁴².

Central to enabling the barrier function of skin are the skin ceramides¹². Ceramide homeostasis of the skin depends on a dynamic balance between biosynthetic and catabolic pathways. The observation that biofilm infection by PA_{wt}, but not PA_{ΔCer}, compromises barrier function of the repaired skin provides direct evidence implicating ceramide depletion in impaired restoration of barrier function during healing. CerS3 is recognized as the primary catalyst of long chain cutaneous ceramide synthesis³⁰. This work recognizes biofilm-inducible miR-106b as a post-transcriptional gene silencer of CerS3.

Findings of this study demonstrate that PA leverages host lipids to bolster biofilm formation. Addition of cutaneous porcine lipid augmented biofilm formation in a manner sensitive to delipidation. Lipids *per se* were not the trigger because such augmentation of biofilm was absent with PA_{ΔCer}. Biofilm formation is linked with quorum sensing (QS) pathway of PA⁴³. The current work demonstrates that ceramide breakdown products are capable of inducing *SphR*. During antibiotic resistance of PA, *SphR* is involved in quorum sensing VqSM-SphR interaction⁴⁴. This pathway represents a plausible mechanism by which skin lipids may induce QS. In transcriptional regulation of host skin lipids, peroxisome proliferator-activated receptor PPAR δ plays a central role⁴⁵. This hub emerged as a central player in the paradigm unveiled by the findings of this study. Basal PPAR δ activity in the skin is driven by ceramides³¹. The PA biofilm dependent amplification loop, as described above, depleted skin ceramides thus lowering PPAR δ activity. As part of that loop as ceramides were catabolized to sphingosine, S-1-P was produced. S-1-P epigenetically silenced PPAR δ expression. It is known that quorum-sensing molecule such 2-aminoacetophenone or other unrelated pathogen associated molecules of PA can regulate the host epigenome through HDAC1-mediated epigenetic reprogramming to enable tolerance of infection⁴⁶. In lung injury secondary to inflammation caused by *P. aeruginosa*, ceramide-derived sphingosine and S1P are directly implicated⁴⁷. Interestingly, ceramide can also act as antimicrobials. Sphingosine effectively killed *S. aureus*, *Streptococcus pyogenes*, *Micrococcus luteus*, *Propionibacterium acnes*, *Staphylococcus epidermidis* and moderately killed *P. aeruginosa*⁴⁸. Sphingosine prevented and eliminated *Staphylococcus epidermidis* biofilm on orthopedic implant materials⁴⁹. Sphingosine binds to bacterial membrane cardiolipin and limit growth⁵⁰. Bacterial growth retardation is inherent to biofilm formation⁵¹. Consistently, the finding of this work reports that elevated S-1-P, a derivative of sphingosine, is associated with higher biofilm formation.

A third mechanism to down-regulate PPAR δ was contributed by PA biofilm inducible miR-106b. This may be viewed as a well-coordinated effort by PA biofilm to disable skin PPAR δ and therefore hijack host metabolic processes to augment biofilm fate. Of particular interest is the observation that this entire cascade of events is triggered by host lipids. As it relates to the functional significance of PPAR δ in barrier function of the skin, it is known that topical application of an agonist of PPAR δ accelerates restoration of such function following injury⁵².

The ATP-binding cassette (ABC) transporter ABCA12, transcriptionally regulated by PPAR δ , encodes a highly conserved group of proteins involved in active transport of a variety of lipids across biological membranes⁵³. In epidermal keratinocytes, PPAR δ upregulates ABCA12³⁶. Loss of skin wound-site PPAR δ in response to PA biofilm infection was associated with compromised ABCA12 expression. At the wound-site, where covering of the defect with

repaired skin has been achieved it was noted that this ABCA12-deficient epidermis was also compromised in abundance of lipids. Such pathological manifestation has been also reported in congenital ichthyoses where low ABCA12 is associated with compromised skin barrier⁵⁴. This is consistent with our previously report demonstrating that wounds with a history of biofilm infection appears closed but is not functionally closed as the site is deficient in barrier function¹⁻³. Closed wound-site with a history of biofilm infection, featuring compromised barrier function, is known to biomechanically deficient with weak tensile strength³. This observation, taken together with the report that skin deficient in barrier function act as window allowing entry of pathogenic allergens to the body⁴¹, points towards the hypothesis that such affected site may be prone to wound recidivism and other threats to general health³.

In summary, this work reports that in the setting of cutaneous wound, pathogenic PA biofilm formation relies on the theft of host lipid factors which the bacteria use to turn on and sustain its bolstered ceramidase system which is otherwise weak. PA biofilm formation was highly responsive to its microenvironment such that in the context of skin wounds it utilized ceramide breakdown products to augment biofilm aggregates. This process was initiated by a massive induction of bacterial ceramidase in response to host lipids. Downstream products of such metabolism such as sphingosine and S-1-P were directly implicated in induction of ceramidase and inhibition of PPAR δ , respectively. PA biofilm also silenced PPAR δ *via* induction of miR-106b. Low PPAR δ limits ABCA12 expression resulting in disruption of skin lipid homeostasis. Barrier function of the skin was thus compromised. The significance of such defect in the functional deficiency of the skin with respect to risk of infection and wound recurrence warrant further consideration.

ACKNOWLEDGEMENTS

This work was supported by the US National Institutes of Health grants R01DK114718 to SR, NIH R01NS085272 to SK; NIH NR015676 and U01DK119099 to SR, GG and CKS; NIH R01GM108014, R01NS042617, R01DK125835, R01DK128845 and U24DK122927 to CKS. The authors acknowledge the Integrated Nanosystems Development Institute (INDI) for use of their JEOL7800F Field Emission Scanning Electron Microscope. We thank Metabolite Profiling Facility, Purdue University. We thank Metabolon Inc. for metabolic profiling of human wound fluids. We thank Dr. Bert Vogelstein for generous donation of PPAR δ promoter reporter plasmid. We thank Dr. Daniel Wozniak, The Ohio State University for providing the *Acinetobacter baumannii* strain. We thank Dr. Makoto Ito, Kyushu University, Fukuoka, Japan for providing the PA_{wt} and PA Δ Cer strains. All of the work was conducted in USA. Dr. El-Masry is on leave from Zagazig University for surgeon scientist training with CKS. We thank Jessica Smith, Indiana University and Elizabeth Schwab, The Ohio State University for their support with the porcine experiments.

AUTHOR CONTRIBUTIONS

CKS, MS and NG conceived and designed the work. MS, NG, DSW, SMS, AD, KS, MEM, HI, KY and MK participated in the data acquisition, interpretation and analysis. MS, NG and CKS wrote the manuscript. MS, NG, GG, SK, SR and CKS were involved in revising the

manuscript critically for important intellectual content. All authors have reviewed the manuscript.

DECLARATION OF INTERESTS

The authors declare no competing interests

REFERENCES

1. Barki KG, Das A, Dixith S, et al. Electric Field Based Dressing Disrupts Mixed-Species Bacterial Biofilm Infection and Restores Functional Wound Healing. *Ann Surg* 2019; 269(4):756-766.
2. Roy S, Elgharably H, Sinha M, et al. Mixed-species biofilm compromises wound healing by disrupting epidermal barrier function. *J Pathol* 2014; 233(4):331-343.
3. Roy S, Santra S, Das A, et al. Staphylococcus aureus Biofilm Infection Compromises Wound Healing by Causing Deficiencies in Granulation Tissue Collagen. *Ann Surg* 2020; 271(6):1174-1185.
4. Wolcott R, Dowd S. The role of biofilms: are we hitting the right target? *Plast Reconstr Surg* 2011; 127 Suppl 1:28S-35S.
5. Fazli M, Bjarnsholt T, Kirketerp-Moller K, et al. Nonrandom distribution of Pseudomonas aeruginosa and Staphylococcus aureus in chronic wounds. *J Clin Microbiol* 2009; 47(12):4084-9.
6. Ruffin M, Brochiero E. Repair Process Impairment by Pseudomonas aeruginosa in Epithelial Tissues: Major Features and Potential Therapeutic Avenues. *Front Cell Infect Microbiol* 2019; 9:182.
7. Balasubramanian D, Schneper L, Kumari H, et al. A dynamic and intricate regulatory network determines Pseudomonas aeruginosa virulence. *Nucleic Acids Res* 2013; 41(1):1-20.
8. Jesaitis AJ, Franklin MJ, Berglund D, et al. Compromised host defense on Pseudomonas aeruginosa biofilms: characterization of neutrophil and biofilm interactions. *J Immunol* 2003; 171(8):4329-39.
9. Rumbaugh KP. Genomic complexity and plasticity ensure Pseudomonas success. *FEMS Microbiol Lett* 2014; 356(2):141-3.
10. Moser C, Pedersen HT, Lerche CJ, et al. Biofilms and host response - helpful or harmful. *APMIS* 2017; 125(4):320-338.
11. Okino N, Tani M, Imayama S, et al. Purification and characterization of a novel ceramidase from Pseudomonas aeruginosa. *J Biol Chem* 1998; 273(23):14368-73.
12. Coderch L, Lopez O, de la Maza A, et al. Ceramides and skin function. *Am J Clin Dermatol* 2003; 4(2):107-29.

13. Baker LY, Hobby CR, Siv AW, et al. Pseudomonas aeruginosa responds to exogenous polyunsaturated fatty acids (PUFAs) by modifying phospholipid composition, membrane permeability, and phenotypes associated with virulence. *BMC Microbiol* 2018; 18(1):117.
14. Bhattacharya M, Berends ETM, Chan R, et al. Staphylococcus aureus biofilms release leukocidins to elicit extracellular trap formation and evade neutrophil-mediated killing. *Proc Natl Acad Sci U S A* 2018; 115(28):7416-7421.
15. Ohnishi Y, Okino N, Ito M, et al. Ceramidase activity in bacterial skin flora as a possible cause of ceramide deficiency in atopic dermatitis. *Clin Diagn Lab Immunol* 1999; 6(1):101-4.
16. Contaifer D, Jr., Carl DE, Warncke UO, et al. Unsupervised analysis of combined lipid and coagulation data reveals coagulopathy subtypes among dialysis patients. *J Lipid Res* 2017; 58(3):586-599.
17. Bligh EG, Dyer WJ. A rapid method of total lipid extraction and purification. *Can J Biochem Physiol* 1959; 37(8):911-7.
18. Gajenthra Kumar N, Contaifer D, Jr., Baker PRS, et al. Untargeted lipidomic analysis to broadly characterize the effects of pathogenic and non-pathogenic staphylococci on mammalian lipids. *PLoS One* 2018; 13(10):e0206606.
19. Zhao G, Hochwalt PC, Usui ML, et al. Delayed wound healing in diabetic (db/db) mice with Pseudomonas aeruginosa biofilm challenge: a model for the study of chronic wounds. *Wound Repair Regen* 2010; 18(5):467-77.
20. Greenspan P, Mayer EP, Fowler SD. Nile red: a selective fluorescent stain for intracellular lipid droplets. *J Cell Biol* 1985; 100(3):965-73.
21. Deng B, Ghatak S, Sarkar S, et al. Novel Bacterial Diversity and Fragmented eDNA Identified in Hyperbiofilm-Forming Pseudomonas aeruginosa Rugose Small Colony Variant. *iScience* 2020; 23(2):100827.
22. Singh K, Pal D, Sinha M, et al. Epigenetic Modification of MicroRNA-200b Contributes to Diabetic Vasculopathy. *Mol Ther* 2017; 25(12):2689-2704.
23. Jennings LK, Storek KM, Ledvina HE, et al. Pel is a cationic exopolysaccharide that cross-links extracellular DNA in the Pseudomonas aeruginosa biofilm matrix. *Proc Natl Acad Sci U S A* 2015; 112(36):11353-8.
24. Okino N, Ito M. Molecular mechanism for sphingosine-induced Pseudomonas ceramidase expression through the transcriptional regulator SphR. *Sci Rep* 2016; 6:38797.
25. Inoue H, Someno T, Kato T, et al. Ceramidastin, a novel bacterial ceramidase inhibitor, produced by Penicillium sp. Mer-f17067. *J Antibiot (Tokyo)* 2009; 62(2):63-7.
26. Solano C, Echeverz M, Lasa I. Biofilm dispersion and quorum sensing. *Curr Opin Microbiol* 2014; 18:96-104.
27. Wurtzel O, Yoder-Himes DR, Han K, et al. The single-nucleotide resolution transcriptome of Pseudomonas aeruginosa grown in body temperature. *PLoS Pathog* 2012; 8(9):e1002945.
28. Allegretta G, Maurer CK, Eberhard J, et al. In-depth Profiling of MvfR-Regulated Small Molecules in Pseudomonas aeruginosa after Quorum Sensing Inhibitor Treatment. *Front Microbiol* 2017; 8:924.

29. Das T, Kutty SK, Kumar N, et al. Pyocyanin facilitates extracellular DNA binding to *Pseudomonas aeruginosa* influencing cell surface properties and aggregation. *PLoS One* 2013; 8(3):e58299.
30. Mullen TD, Hannun YA, Obeid LM. Ceramide synthases at the centre of sphingolipid metabolism and biology. *Biochem J* 2012; 441(3):789-802.
31. Jiang YJ, Uchida Y, Lu B, et al. Ceramide stimulates ABCA12 expression via peroxisome proliferator-activated receptor δ in human keratinocytes. *J Biol Chem* 2009; 284(28):18942-52.
32. Ebenezer DL, Fu P, Suryadevara V, et al. Epigenetic regulation of pro-inflammatory cytokine secretion by sphingosine 1-phosphate (S1P) in acute lung injury: Role of S1P lyase. *Adv Biol Regul* 2017; 63:156-166.
33. Feingold KR. Thematic review series: skin lipids. The role of epidermal lipids in cutaneous permeability barrier homeostasis. *J Lipid Res* 2007; 48(12):2531-46.
34. Jungersted JM, Hellgren LI, Jemec GB, et al. Lipids and skin barrier function--a clinical perspective. *Contact Dermatitis* 2008; 58(5):255-62.
35. Feingold KR, Elias PM. Role of lipids in the formation and maintenance of the cutaneous permeability barrier. *Biochim Biophys Acta* 2014; 1841(3):280-94.
36. Jiang YJ, Lu B, Kim P, et al. PPAR and LXR activators regulate ABCA12 expression in human keratinocytes. *J Invest Dermatol* 2008; 128(1):104-9.
37. Toledo A, Benach JL. Hijacking and Use of Host Lipids by Intracellular Pathogens. *Microbiol Spectr* 2015; 3(6).
38. Grassme H, Jendrossek V, Riehle A, et al. Host defense against *Pseudomonas aeruginosa* requires ceramide-rich membrane rafts. *Nat Med* 2003; 9(3):322-30.
39. Dar HH, Tyurina YY, Mikulska-Ruminska K, et al. *Pseudomonas aeruginosa* utilizes host polyunsaturated phosphatidylethanolamines to trigger theft-ferroptosis in bronchial epithelium. *J Clin Invest* 2018; 128(10):4639-4653.
40. Gordillo GM, Bernatchez SF, Diegelmann R, et al. Preclinical Models of Wound Healing: Is Man the Model? Proceedings of the Wound Healing Society Symposium. *Adv Wound Care (New Rochelle)* 2013; 2(1):1-4.
41. De Benedetto A, Kubo A, Beck LA. Skin barrier disruption: a requirement for allergen sensitization? *J Invest Dermatol* 2012; 132(3 Pt 2):949-63.
42. Agrawal R, Woodfolk JA. Skin barrier defects in atopic dermatitis. *Curr Allergy Asthma Rep* 2014; 14(5):433.
43. De Kievit TR, Gillis R, Marx S, et al. Quorum-sensing genes in *Pseudomonas aeruginosa* biofilms: their role and expression patterns. *Appl Environ Microbiol* 2001; 67(4):1865-73.
44. Liang H, Deng X, Li X, et al. Molecular mechanisms of master regulator VqsM mediating quorum-sensing and antibiotic resistance in *Pseudomonas aeruginosa*. *Nucleic Acids Res* 2014; 42(16):10307-20.

45. Sertznig P, Seifert M, Tilgen W, et al. Peroxisome proliferator-activated receptors (PPARs) and the human skin: importance of PPARs in skin physiology and dermatologic diseases. *Am J Clin Dermatol* 2008; 9(1):15-31.
46. Bandyopadhyaya A, Tsurumi A, Maura D, et al. A quorum-sensing signal promotes host tolerance training through HDAC1-mediated epigenetic reprogramming. *Nat Microbiol* 2016; 1:16174.
47. Ebenezer DL, Berdyshev EV, Bronova IA, et al. Pseudomonas aeruginosa stimulates nuclear sphingosine-1-phosphate generation and epigenetic regulation of lung inflammatory injury. *Thorax* 2019; 74(6):579-591.
48. Bibel DJ, Aly R, Shinefield HR. Antimicrobial activity of sphingosines. *J Invest Dermatol* 1992; 98(3):269-73.
49. Beck S, Sehl C, Voortmann S, et al. Sphingosine is able to prevent and eliminate Staphylococcus epidermidis biofilm formation on different orthopedic implant materials in vitro. *J Mol Med (Berl)* 2020; 98(2):209-219.
50. Verhaegh R, Becker KA, Edwards MJ, et al. Sphingosine kills bacteria by binding to cardiolipin. *J Biol Chem* 2020; 295(22):7686-7696.
51. Donlan RM, Costerton JW. Biofilms: survival mechanisms of clinically relevant microorganisms. *Clin Microbiol Rev* 2002; 15(2):167-93.
52. Schmuth M, Haqq CM, Cairns WJ, et al. Peroxisome proliferator-activated receptor (PPAR)-beta/delta stimulates differentiation and lipid accumulation in keratinocytes. *J Invest Dermatol* 2004; 122(4):971-83.
53. Borst P, Elferink RO. Mammalian ABC transporters in health and disease. *Annu Rev Biochem* 2002; 71:537-92.
54. Akiyama M. The roles of ABCA12 in epidermal lipid barrier formation and keratinocyte differentiation. *Biochim Biophys Acta* 2014; 1841(3):435-40.

Figure Legends

Fig. 1 Inducible Bacterial Ceramidases Deplete Host Cutaneous Ceramide

(A) Schematic presentation of the timeline of porcine model of chronic wound biofilm infection. (B) Induction of bacterial ceramidase (*bcdase*) in biofilm infected porcine wounds. Real-time qPCR analysis of *bcdase* expression spontaneously infected (SI) and wild type *P. aeruginosa* (PA_{wt}) infected porcine wound epidermis (d7 post-infection) collected by laser capture micro-dissection (LCM). Data presented as mean \pm SEM, (n=5). (C) $PA_{\Delta cer}$ biofilm was deficient in secreted *bcdase* activity. Data presented as mean \pm SEM, (n=6). See Fig. S1A, <http://links.lww.com/SLA/D496> for gene *bcdase* expression data. [NBD-CER - C12-NBD-Ceramide, NBD-DA - NBD-dodecanoic acid]. (D-E) Depletion of ceramide in porcine wounds infected with PA_{wt} biofilm compared to SI or wounds infected with ceramidase mutant of *P. aeruginosa* ($PA_{\Delta cer}$). Porcine d56 wound tissues were immuno-stained with anti-ceramide (red) antibody and DAPI (blue). Data presented as mean \pm SEM, (n=6). Scale bar = 500 μ m and zoomed inset = 50 μ m. (F) Depletion of ceramides in porcine skin lipid exposed to PA_{wt} , or $PA_{\Delta cer}$ as measured by LC/MS/MS targeted-lipidomic approach. Same skin lipid not exposed to any bacteria was used as sham control. Hierarchical Cluster Analysis revealed down-regulation of 19 species of ceramide in the skin lipid (n=6). Individual ceramides that were specifically affected are illustrated in **supplementary figure 2**, <http://links.lww.com/SLA/D496>. (G) Principal component analyses of the abundance of cutaneous ceramides in response to PA_{wt} or $PA_{\Delta cer}$ exposure. Sham and $PA_{\Delta cer}$ clusters were not statistically different. This combined group was statistically distinct from cutaneous ceramide levels in response to PA_{wt} . (H) Complete re-epithelization following SI, PA_{wt} and $PA_{\Delta cer}$ biofilm infection. Hematoxylin-Eosin staining shown. Scale bar = 500 μ m and zoomed inset = 50 μ m. Macroscopic digital planimetry shown in **supplementary figure 3M**, <http://links.lww.com/SLA/D496>. (I) Functional restoration of barrier function of cutaneous wounds, measured by trans-epidermal water loss (TEWL), was compromised following PA_{wt} biofilm infection. Data presented as mean \pm SEM (n=6). † p<0.05 as compared to $PA_{\Delta cer}$; and *p < 0.05 as compared to SI.

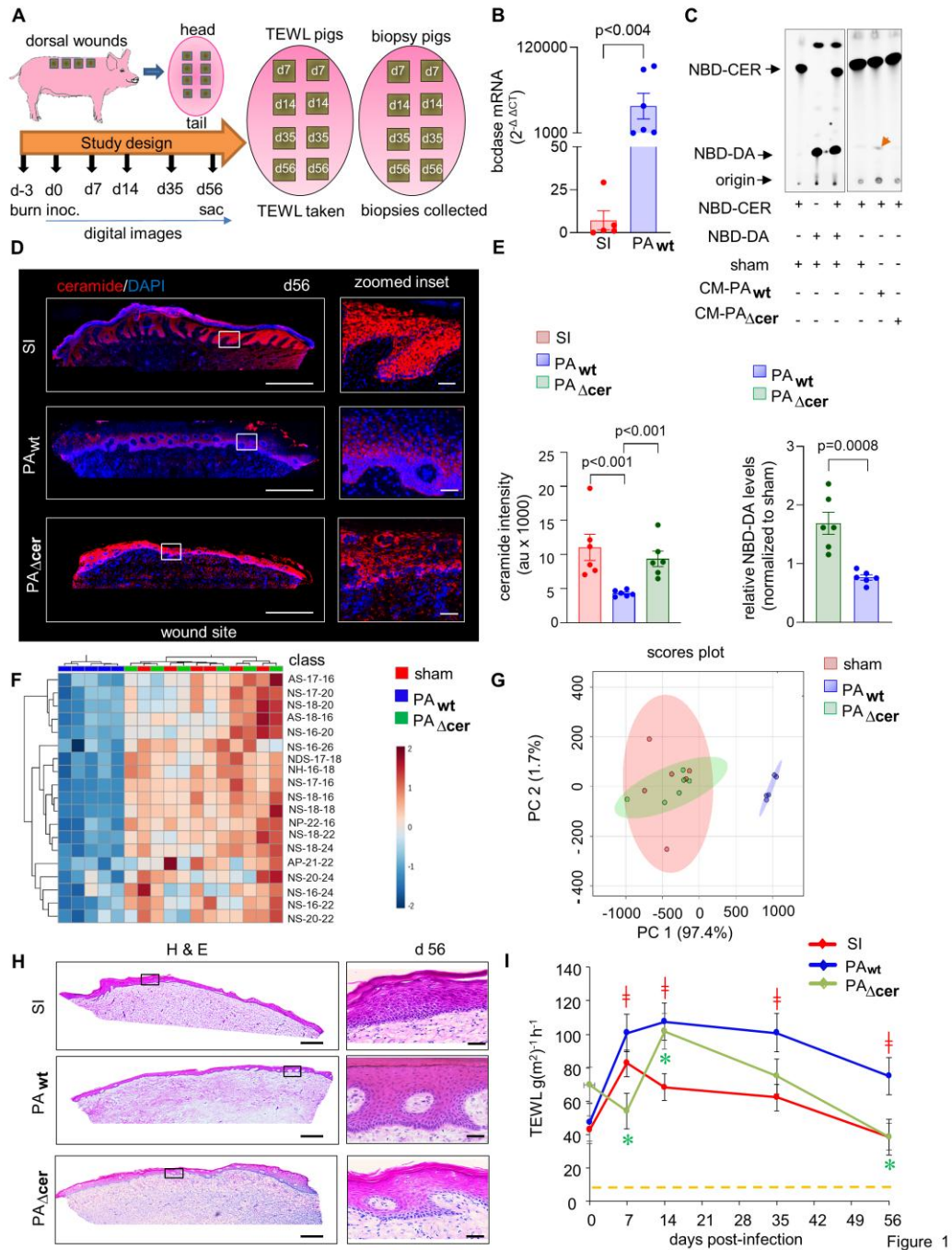


Fig.2 Host Lipids Facilitate PA_{wt} Biofilm Aggregate Formation

(A-E) (i) Cutaneous lipids induced biofilm aggregate formation in an *in vitro* polycarbonate membrane biofilm system after 24h of inoculation. **A**, PA_{wt} + vehicle (PBS); **B**, PA_{wt} + skin lipids; **C**, PA_{wt} + depleted lipids; **D**, PA_{Δcer} + vehicle (PBS) **E**, PA_{Δcer} + skin lipids. (ii) Increased abundance of EPS in PA_{wt} biofilm in response to host lipids as recorded in SEM images. Thick EPS is marked by yellow circles. EPS fibers are marked by yellow arrows. Scale bar = 100 nm, 30,000x magnification. Larger SEM fields are presented as **supplementary figure 4**, <http://links.lww.com/SLA/D496>. (iii) Host lipids induced biofilm aggregate formation in PA_{wt} as measured by wheat germ agglutinin (WGA) staining. Scale bar = 10 μm . (iv) Respective 3D

reconstructed images of (iii). (F) Quantification of biofilm aggregates using WGA staining as shown in (iii). Data presented as mean \pm SEM, n=10. (G-H) Host lipids induce biofilm gene expression in pathogen PA_{wt}. Data presented as mean \pm SEM, (n=5).

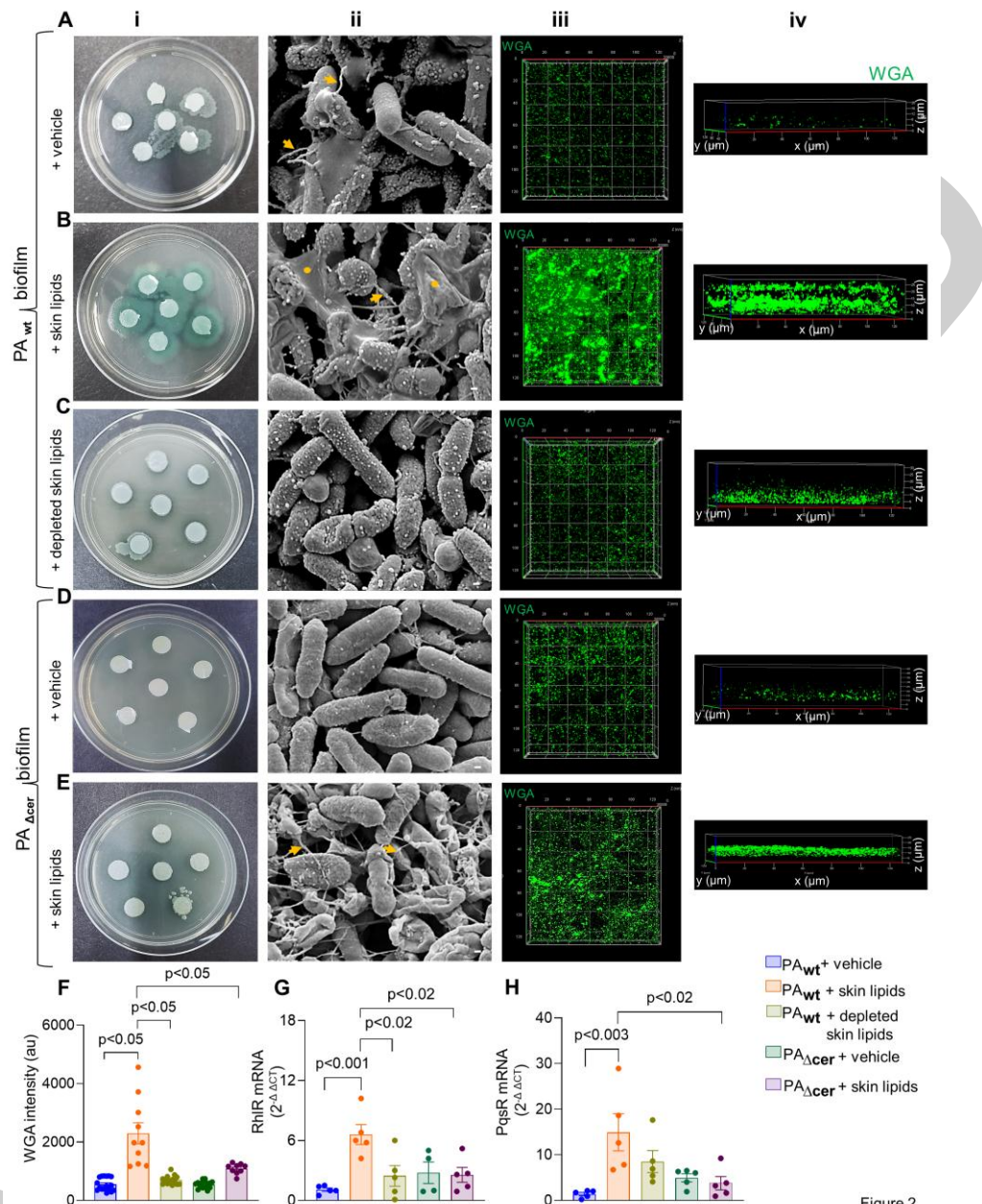


Figure 2

Fig. 3 Biogenesis of Host Long Chain Ceramides is Compromised Under Conditions of PA_{wt} Biofilm Infection

(A) Long chain ceramide biogenesis pathways outlined. (B) Downregulation of CerS3 in wound-site skin tissue infected with PA_{wt} compared to SI or PA_{Δcer} measured by qPCR. Data presented as mean \pm SEM (n = 5-7). (C) PA_{wt} lowered the levels of the levels of dihydroceramide (C18DHCer) in skin lipids. Measured by LC/MS/MS targeted lipidomic approach. Data are presented as mean \pm SEM (n = 6). (D) Wound fluid collection from chronic wound patients who underwent negative pressure wound therapy (NPWT) as part of standard

of care. (E-F) Lower levels of dihydroceramide in cyclic diGMP-rich human wound fluid. cyclic di-GMP is a marker of PA biofilm infection (n=5). (G) Biofilm induced miR-106b targets host CerS3 (H) Elevated miR-106b in human keratinocytes (HK) infected with PA_{wt} biofilm as measured by qPCR. Data presented as mean ± SEM (n=7-10). (I-J) miR-106b is predicted to target the 3'-UTR of CerS3 position 331-355 according to RNAHybrid™ algorithm. (K) miR-106b silenced pmiR-Target-Cers-3'-UTR in human keratinocytes (HK). FL, Firefly luciferase; RL, Renilla luciferase. Data are mean ± SEM (n=4). (L) miR-106b silenced CerS3 protein expression in human keratinocytes (HK). Data are presented as mean ± SEM (n=6).

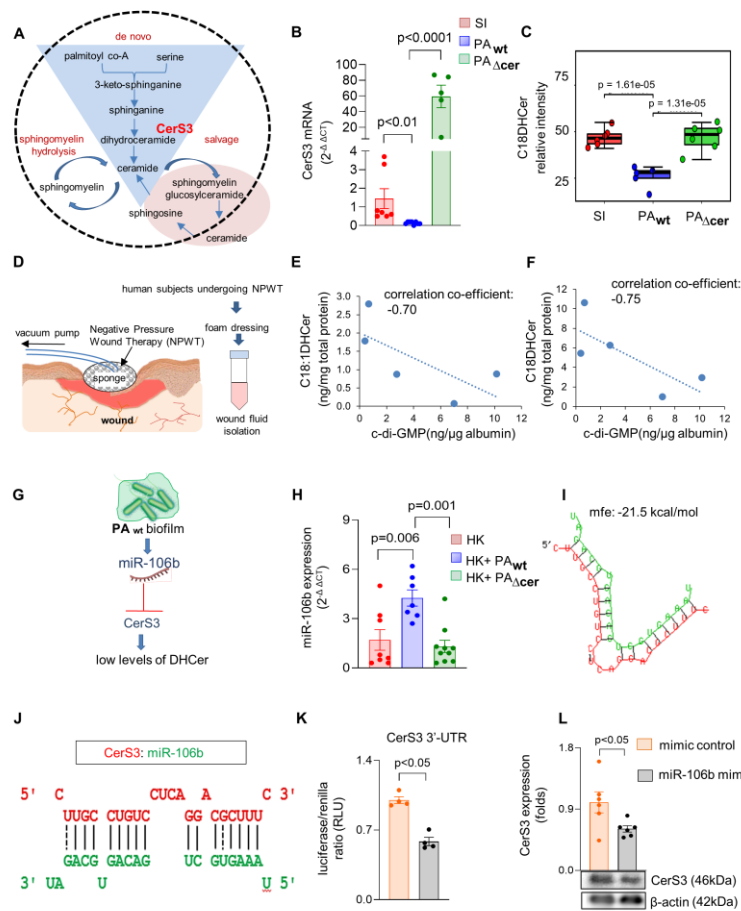


Figure 3

Fig. 4 Wound-Site Skin PPAR δ Expression is Downregulated in Response to PA_{wt} Biofilm Infection

(A) PA_{wt} biofilm compromises host cutaneous PPAR δ expression. (B-C) Loss of cutaneous host PPAR δ in porcine wounds infected with PA_{wt} compared to SI or PA Δ cer wounds. Porcine wound sections were immunostained with anti-PPAR δ (green) and DAPI (blue). Porcine wound section images (scale bar = 500 μ m) and corresponding zoomed inset (scale bar = 50 μ m) showed PPAR δ protein expression. Data presented as mean ± SEM (n = 5-6). (D) Lower expression of PPAR δ in PA_{wt} infected wound tissue. Whole tissue homogenate was used for

analysis. Data presented as mean \pm SEM, (n = 3-8). (E) Lower expression of PPAR δ protein in human keratinocytes (HK) infected with PA_{wt} biofilm. Data presented as mean \pm SEM (n=5). (F) Ceramidastin attenuated the negative effects of PA_{wt} biofilm on PPAR δ expression in human keratinocytes. Ceramidastin, 10 μ g/ml. Data presented as mean \pm SEM (n = 6). (G) PPAR δ promoter assay approach. (H) Increased PPAR δ transactivity in human keratinocytes (HK) treated with long chain ceramides (C18 & C24, 5 μ mol/ml). Nuclear extract of the transfected cells treated for 48h were used to measure PPAR δ trans-activity. Data presented as mean \pm SEM (n = 5). (I) Activation of PPAR δ promoter by long chain ceramides as measured by reporter assay. Human keratinocytes (HK) were transfected with PPAR δ promoter along with long chain ceramides (C:18, C:24, 5 μ mol/ml). Data presented as mean \pm SEM (n = 3). (J) Elevated levels of sphingosine-1-phosphate (S-1-P) in PA_{wt} infected wound tissues. Measured by LC/MS/MS targeted lipididomic approach. Cutaneous wound tissue infected with PA_{wt} showed higher levels of S-1-P as compared to SI or PA Δ cer infected wounds. Data presented as mean \pm SEM (n = 6). (K) Down-regulation of PPAR δ gene expression in human keratinocytes (HK) receiving S-1-P (5 μ mol/ml). Data presented as mean \pm SEM (n = 6-7). (L) Region of PPAR δ promoter analyzed through bisulfite genomic sequencing of DNA. Methylation profile of the PPAR δ promoter in human keratinocytes (HK) treated with S-1-P (5 μ mol, 48h). Methylated CpG in black (filled) and unmethylated CpG in white (open). Number of clones = 10 (M) Increased DNA methyl transferase 3B (DNMT3B) activity in human keratinocytes (HK) treated S-1-P (5 μ M, 48h). Data presented as mean \pm SEM (n =4-5).

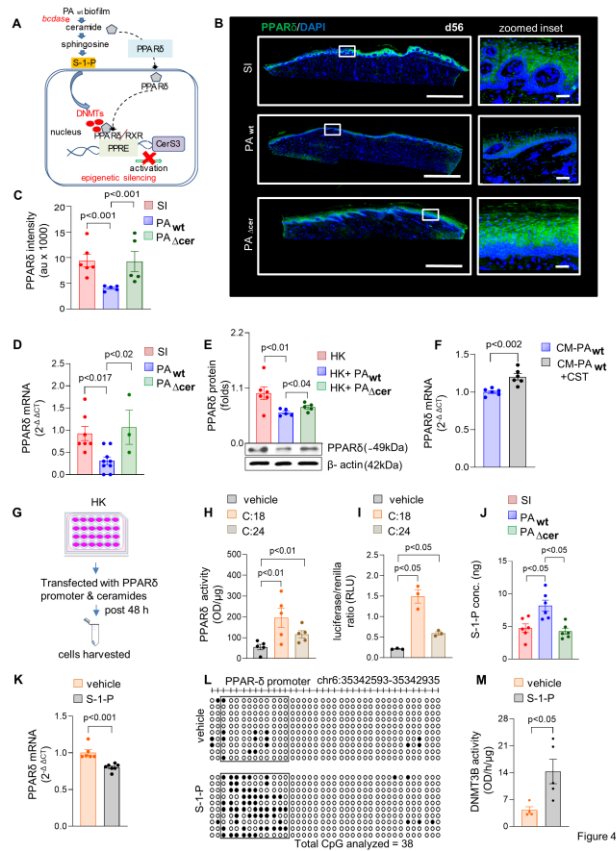


Fig.5 miR-106b Targets PPAR δ in PA_{wt} Biofilm Infected Keratinocytes

(A) RNA HybridTM-based prediction shows that PPAR δ 3'-UTR is a target of miR-106b. (B) PPAR δ downregulation in miR-106b mimic transfected human keratinocytes (HK) as measured by qPCR. Data presented as mean \pm SEM (n=3-4). (C) Downregulated PPAR δ protein in response to miR-106b mimic as measured by Western blot in HK. Data presented as mean \pm SEM (n=6). (D) miR-106b targets PPAR δ 3'UTR as shown by reporter assay. HK were transfected with HmiT013627-MT06- PPAR δ -3'-UTR (NM_006238) along with miR-106b mimic or control mimic. Data presented as mean \pm SEM (n=5).

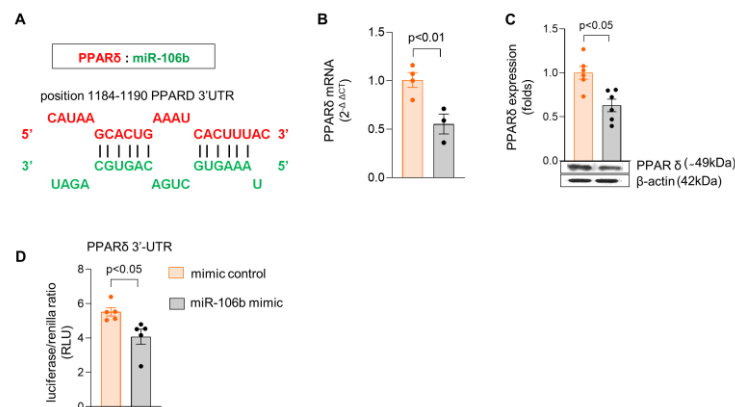


Figure 5

Fig 6. ABCA12 Expression Is Compromised Following PA_{wt} Biofilm Infection

(A) Schematic depiction of the hypothetical pathway. (B-C) Loss of ABCA12 in wound-site epithelium which was infected with PA_{wt} compared to SI or PA Δ cer groups. Scale bar = 500 μ m with corresponding zoomed images of 50 μ m. anti-ABCA12 (green) and DAPI (blue). Data presented as mean \pm SEM (n=5). (D) Downregulation of ABCA12 in porcine wounds infected with PA_{wt} compared to SI or PA Δ cer wounds measured by qPCR. Whole tissue homogenate was used for analysis. Data presented as mean \pm SEM (n = 5-8). (E) Disruption of neutral and polar lipid distribution at the affected wound-site skin. Scale bar = 500 μ m with corresponding zoomed images of 50 μ m. Nile Red staining with DAPI (blue) showing expression of polar lipids (red) and neutral lipids (green). Data presented as mean \pm SEM (n = 5). (F) Ceramidastin

(10 μ g/ml) attenuated biofilm-induced loss of ABCA12 expression in human keratinocytes (HK) as measured by qPCR. Data presented as mean \pm SEM (n = 5-6).

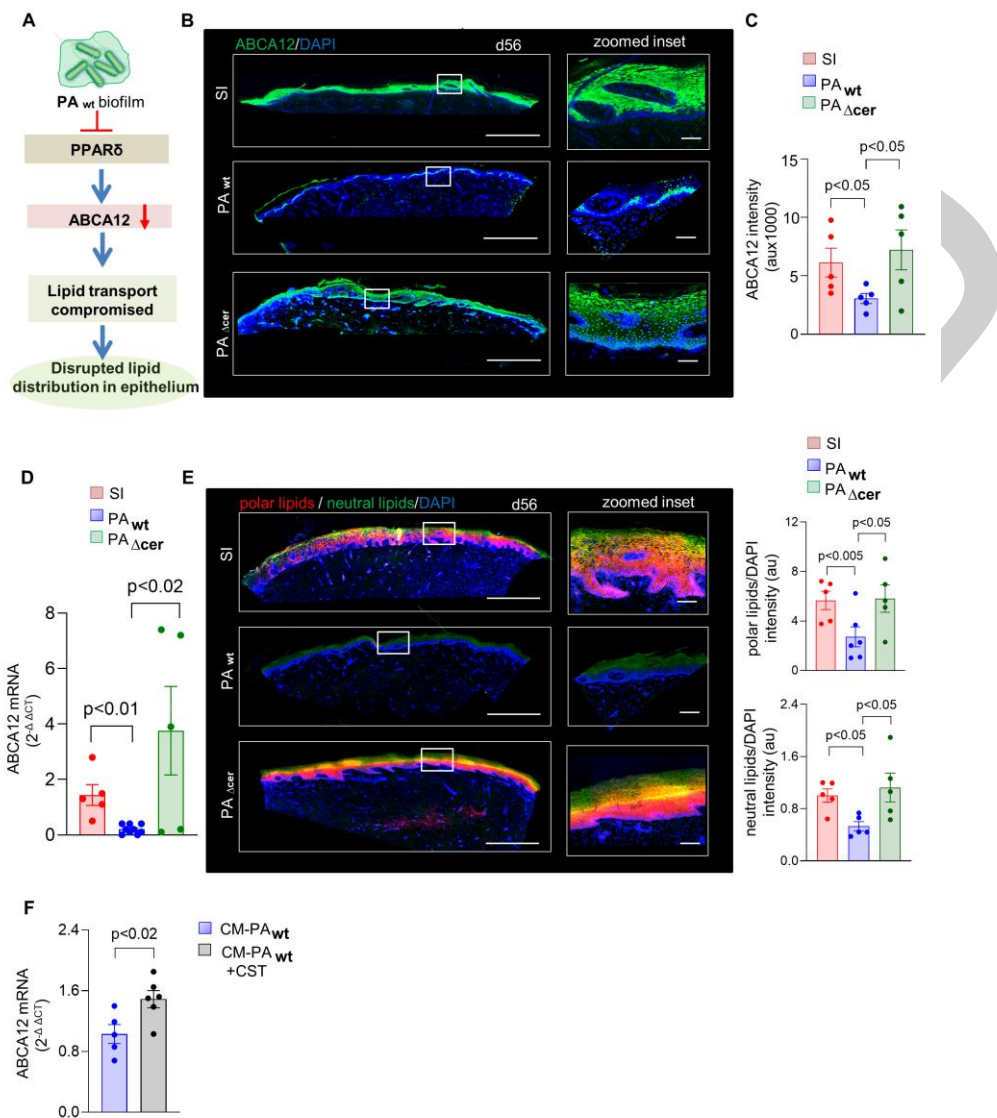


Figure 6

Fig 7. Summary figure

In cutaneous wounds, *Pseudomonas aeruginosa* forms pathogenic theft biofilm. Such biofilm severity relies on the theft of host lipids (ceramides) causing potent induction of bacterial ceramidase (bcdase). Skin ceramide biosynthesis is impaired by post-transcriptional gene silencing of CerS3 by biofilm-inducible miR106b. The limited ceramide pool, thus available as inducer of inducers of PPAR δ , is threatened by elevated biofilm bcdase. Thus expression of PPAR δ , a major regulator of skin lipid homeostasis, is blunted. PPAR δ faces a second line of attack in the form of epigenetic silencing by both biofilm-inducible miR-106b as well as S-1-P. Such loss of PPAR δ compromised downstream genes including cutaneous lipid transporter ABCA12. Taken together, biofilm disrupts skin lipid homeostasis in a way that the site of wound repair cannot restore barrier function, a marker of functional wound healing.

Pseudomonas aeruginosa Theft Biofilm

